J.Soil Sci. and Agric. Eng., Mansoura Univ., Vol. 8 (6): 245 - 256 , 2017

Utilization of Greenhouse (Lean-to Structural Frame) as a Solar Dryer for Drying Lemon Fruits
Part I: Drying Process under High Air Temperature.

Abdellatif, S. M. ; A. T. Mohmed and Ghada A. Mosad
Dept. of Agricultural Engineering, Faculty of Agric. Mansoura University

ABSTRACT

A solar lean-to greenhouse dryer was designed, constructed and tested for drying lemon fruits at the experiments and researches field, Faculty of Agriculture, Mansoura University (latitude and longitude angles, respectively, are 31.04°N and 31.35°E, and 6.72 m mean altitude above the sea level). In this study a new concept has been taken into consideration to maximize the greenhouse effect (thermal trapping) by using architectural form of lean-to greenhouse structural frame. The experimental work was carried out from 21st to 26th of August 2016. The obtained results showed that, using the northern wall reflector caused in increasing both the intensity of solar radiation inside the dryer and the indoor air temperature by 36.30% and 60.90%, respectively. The daily average solar radiation incident outside and inside the solar dryer were 5.188 and 3.383 kWh, respectively with effective transmittance of 65.21%. Using the northern reflector wall increased the daily average indoor solar radiation by 36.12%. The daily average outdoor and indoor air temperatures were 30.1 and 48.4ºC, respectively. Accordingly, the solar dryer increased the indoor air temperature over the outdoor by 60.80%. These conditions of solar dryer caused in decreasing the daily average air relative humidity from 67.31 to 28.38% with reduction percentage of 38.93%. Three different shapes of lemon fruits (slices, half and whole lemon) was dried from initial moisture content of 87.04% (w.b.) to the final moisture of 17.30, 17.38 and 17.69% (w.b) within 3, 5, and 6 days, respectively.

Keywords: Lean-to greenhouse, solar dryer, renewable energy, and lemon fruits.

INTRODUCTION

Solar is one of the renewable and sustainable sources of power that attracted a large community of researchers from all over the world. This is largely due to its abundant in both direct and indirect form. As such the development of efficient and inexpensive equipment for the drying of agricultural products using solar power evolved thereby improving the quality of the products as well as improving the quality of life. The use of solar dryers in the drying of agricultural products can significantly reduce or eliminate product wastage, food poisoning at sometime enhance productivity of the farmers towards better revenue derived (Toshniwal and Karale, 2013). Traditional open-sun drying mode is used for drying agricultural products since many thousands of years. However, the drying rate by this mode is mainly controlled by several outer parameters such as solar radiation intensity, ambient air temperature, wind speed, and air relative humidity and inner parameters such as initial moisture content, type of agricultural products, and the mass of product per area of exposing (Jain and Tiwari, 2004). There are considerable advantages with this mode of drying due to the resource of energy is renewable. Nevertheless, it does not allow for obtaining a desirable level and reproducible product quality, basically because of the inherent limitation in controlling the drying process.

Several solar dryers have been designed, constructed, and functioned as an alternative system to the traditional open-sun drying for drying different agricultural products. Drying temperature is a major deciding factor, which mainly determines the quality of the dried product. High drying temperature may impair the germination capacity of seeds and also can damage the product by changing its chemical combination of the product. Lower drying temperature may lead to longer drying time which may lead to microbial contamination. The drying temperature should provide and maintain to the permissible level so that the drying will not damage the product (Aravindh and Sreekumar, 2015). In solar drying of agricultural products, the moisture is removed by the solar heated air having temperature ranged between 50 to 60°C. Solar drying under controlled conditions of temperature and moisture removing rate ensures perfect drying and desirable product quality. The percentage of moisture content in the agricultural products is varied from product to product. For drying different moisture content products, the drying systems are usually classified as low and high temperature operated drying systems. In low temperature operated drying system, the moisture content of the product is brought into equilibrium condition by drying air using proper ventilation. High temperature drying systems are used when fast drying rate is required for high moisture content products (Kumar *et al.,* 2016). The majority of food can be dried at a mean temperature of 60ºC. Some products need lower drying temperatures at the beginning, i.e., apricots, and after being semi-dried temperature can be raised up to certain suitable point. This technique helps to keep the skin of the crop soft, as in many cases higher temperatures harden this skin (Belessiotis and Delyannis, 2011).

Lemons (Citrus Limon) are nutritious fruit with a myriad of health benefits. They boast one of the nature's highest Vitamin C concentrations, total Phenolics content (TPC) and a unique flavour and aroma. Vitamin C is essential for a strong immune system and hence prevents the illness such as flu, colds, and recurrent ear infections. Moreover, several researchers (Ramful *et al.,* 2011, Frei *et al.,* 2012 and many others) have been revealed that consumption of fruits with higher content of Vitamin C lower one's risk of heart diseases and strokes and reduce the symptoms of arthritis. On the other hand, total Phenolics content in lemons demonstrates plenty of biological properties including anti-allergen, anti-mutation effects, and anti-atherosclerosis. Nowadays, dried lemons are a major exported product of Egypt. The total planted area of lemon trees is almost 26,757 feddan which annually producing about 280,641 tons of which 80% are consumed as fresh fruits in miscellaneous purposes. About 20% of the total production of fresh lemons is dried using open-air drying in the sun at new valley and exported the dried product into the Gulf countries. A trial closed-type solar dryer connected to photovoltaic system was developed and functioned for drying lemon slices by Chen *et al*. (2005). The obtained data of dried lemon slices using this type of solar dryer were compared with hot air drying at 60ºC.

They revealed that, the dried lemon slices using the closed-type solar dryer had a highly level of quality in terms of sensory parameters.

The main goal of this research work is to utilize solar energy for drying lemon fruits which is one of the citrus yield species. The objective of this study was to test and examine the performance of solar dryer for drying three different shapes of lemon fruits (slices, half fruit, and whole fruit) during August 2016. Heat energy balance was also executed during the experimental period. Thermal efficiency of solar dryer was also tested.

MATERIALS AND METHODS

Solar Dryer

A solar drier (lean-to greenhouse structural frame) having gross dimensions of 5.80 m long, 3.90 m wide, 0.25 m high of curtain wall, 2 m high of vertical wall, 1.42 m high of gable, rafter length of 4.20 m, net floor surface area of 22.62 m^2 and volume of 66.96 m^3 was designed, constructed, and functioned for drying lemon fruits as shown in Fig.1. It was orientated in East-West direction, whereas, the southern section facing upward the sun's rays and the northern section facing into the cold sky. The solar dryer structural frame was formed of firm square iron bars (6 x 6 cm) with 3 mm thick. It was strongly connected to a concrete footing 0.6 m deep. The rafter was inclined at 20º from the horizontal plan (optimum tilt angle during the experimental period) to minimize the side effects of wind load that may below over the roof of drier and to maximize the solar radiation flux incident on the roof of the solar dryer. The floor surface of solar dryer was covered by 10 cm thick of concrete. The drying chamber is made of galvanized steel sheet with a net surface area of 6.25 m^2. The gross dimensions of drying chamber are 5 m long, 1.25 m wide, 0.5 m deep and 0.5 m high from the concrete floor. Air chamber is connected to electric blower at the eastern side by an air duct of 25 cm in diameter as shown in Fig. (2.a). A window (air inlet) having gross dimensions of 70 cm long and 64 cm high for interring drying air is located at the western side. A blower has 10 blades and driven by 2.0 hp electric motor at 1400 rpm, and 220 v was used to draw the drying air from the solar dryer with mass flow rate 0.99021 kg/sec as shown in Fig.(2.b).The outdoor air was drawn in through the air inlet at the top of the front side (western side) of the solar dryer and is heated by the indoor hot objects and the product exposed to solar radiation. Moist air was expelled from the dryer by an extracting blower. From a number of studies it was observed that, researches around the world have only been used the direct transmitted solar radiation from the southern direction for generating the greenhouse effect inside the dryer at which the product is placed. However, a part of solar radiation incident on the transparent north wall is lost to the surrounding environment and is not utilised. In this study a new concept has been taken into consideration to maximize the greenhouse effect using architectural form of lean-to greenhouse dryer. The northern section of solar dryer was vertically constructed of firm iron bars (6 x 6 cm) with gross dimensions of 5.80 m long, 3.42 m high and net surface area of 19.83 m^2. The northern section was covered by 2.0 mm thick nickel-chrome sheet and functioned as a reflector. In this way, product absorbs three components of solar radiation; direct, diffuse, and reflected resulting in increasing the indoor objects (product, concrete floor, structural frame). Accordingly, the indoor air temperature is raised under both natural and forced convection modes. The

southern front walls (vertical and inclined walls) and the two sides (eastern and western walls) were covered with reinforced polycarbonate plates (6 mm thick) in order to create the greenhouse effect inside the dryer. The reinforced polycarbonate (or the multi-wall structure of polycarbonate) offers significant advantages where thermal insulation is a major consider. The hollow form provides excellent insulation characteristics with heat losses and this increase the greenhouse effect inside the solar dryer (Polygal, 2011).

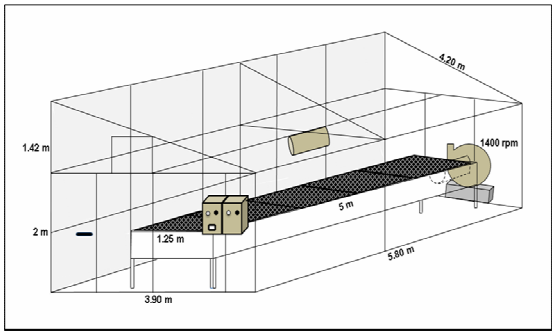

Fig. 1. Schematic diagram of solar lean-to greenhouse dryer.

(a)

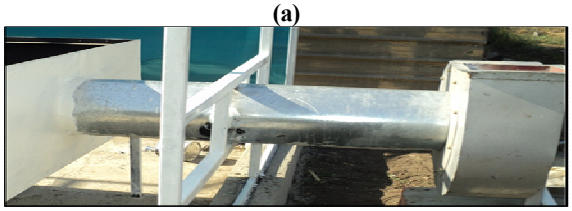

(b)

Fig. 2. (a) Blower driven by an electric motor. (b) Air chamber connected to blower by an air duct.

Solar Radiation Distribution in Solar Dryer

Solar radiation reflected from the northern wall (vertical wall) can be determined by studying the position of the sun which is the geometric relationship between a plane of any particular orientation relative to the earth at any time (whether that plane is fixed or moving relative to the earth) and the incoming beam solar radiation this can be described in terms of several angles. When the sun's rays falling on the reflected wall, there are two dominant angles; the solar altitude angle (Ψ) which is the angle between the sun's rays and the normal to that surface, and the solar zenith angle (z) which is the angle between the sun's rays and the plane of reflected wall as shown in Fig.3. These angles can be computed from the following equations (Duffie and Beckman, 2013):

$$\Psi = \arcsin[\cos\phi \cos\delta \cos\omega + \sin\phi \sin\delta] \quad (1)$$

$$z = \arccos[\cos\phi \cos\delta \cos\omega + \sin\phi \sin\delta] \text{ or } z = 90 - \Psi \quad (2)$$

These angles are depended on latitude angle (φ) which is the angular location north or south of the Equator, and solar declination angle (δ) which is the angular position of the sun at solar noon with respect to the plane of Equator. It depended on the day number from the first of January (n). The solar declination angle can be calculated by the following equation:

$$\delta = 23.45 \sin\left[\frac{360\,(284+n)}{365}\right] \quad (3)$$

Also, solar altitude and zenith angle dependent on the solar hour angle (ω) and solar time considerable. Apparent solar time (AST) generally differs from local standard time (LST) or daylight saving time (DST), and the difference can be significant, particularly when DST is in effect. Because the sun appears to move at the rate of 360º in 24 h, its apparent rate of motion is 4 min per degree of longitude. Thus, the solar hour angle is the angular displacement of the sun east or west of the local meridian due to rotation of the earth on its axis at 15° per hour, morning negative and afternoon is positive. The solar hour angle can be determined from the following equation (ASHREA, 2011):

$$\omega = (LAT - 12) \times 15 \text{ , degree} \quad (4)$$

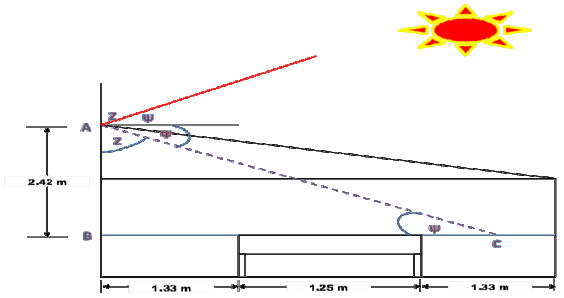

Fig. 3. Schematic diagram show solar altitude angle and zenith angle reflected from the north wall.

The earth's orbital velocity also varies throughout the year, so apparent solar time (AST), as determined by a solar time sundial, varies somewhat from the mean time kept by a clock running at a uniform rate. This variation, called the equation of time. The conversation between local standard time and solar time involves two steps: the equation of time is added to the local standard time, and then a longitude correction is added. This longitude correction is four minutes of time per degree difference between the local (site) longitude and longitude of the local standard meridian for that time zone. Standard meridians are found every 15° from 0° at Greenwich, UK (Greenwich Meridian). Equation (4) relates the local apparent solar time (LAT) to the local standard time (LST) as follows:

$$LAT = LST + \frac{ET}{60} + \frac{LAM - LON}{15} \quad (5)$$

Where:

LAT= apparent solar time, decimal hours
LST= local solar time, decimal hours
ET= equation of time, decimal minutes
LSM= local standard time meridian, decimal degree of arc
LON= local longitude, decimal degree of arc

The equation of time (ET) in minutes can be calculated from the following Equation:

$$ET = 9.87 \sin 2x - 7.53 \sin x - 1.5 \sin x \quad (6)$$

$$x = (n - 81)\frac{360}{365} \quad (7)$$

By determination the value of solar altitude angle (Ψ) the distribution of solar radiation that reflected from the northern wall and reached on the dryer tray can be determined by calculating the length BC.

$$BC = \frac{AB}{\tan\Psi} \quad (8)$$

Experimental Procedure

Fresh lemon fruits were brought from local market during the summer season of 2016 and checked up carefully to discard spoiled ones to prevent contamination of lemon fruits by bacteria or fungi then classified lemons into three groups. The first group was whole lemon fruit, the second group was half lemons, and the third one was lemon slices with 4-6 mm thick as recommended by Sharma *et al.* (2005). A chemical pretreatment is generally applied for whole lemon berry only in order to decrease the skin resistance and hence improving moisture diffusion from these block layers. For the duration of the experimental work, the first section of drying tray inside the solar dryer was loaded with 30 kg of whole lemon berries, 12 kg of half lemons for the second section, and 7 kg of lemon slices (last section). Pretreatment was made before drying process, 30 kg of whole lemon berries were blanched by dipping in boiling solution at 90ºC containing 10 ml/litre of 1% hydroxide sodium (NaOH) solution for 1.5 min for 1 kg of lemon and immediately cooled by immersing in cold water. The objective of this chemical process was to create cracks in the outer layers of the lemon fruits for increasing the drying rate.

Instrumentation and Data Acquisition Unit

Meteorological station (Vantage Pro 2, Davis, USA) located beside the solar dryer (far about 10 m) is used to measure different macroclimate variables such as, the solar radiation flux incident on a horizontal surface, dry-bulb, wet-bulb, and dew-point air temperatures, wind speed and its direction, air relative humidity, and rainfall amounts. These sensors are connected to a data-logger system in order to display and record the data during the experimental period. Microclimate variables of the solar dryer were measured and recorded at height of 2 m above the concrete floor level using data-logger (Watch-dog, 1000 series, USA). These microclimate variables included the solar radiation flux incident on a horizontal surface and on a vertical surface parallel to the northern reflected wall using two disk-solarimeters, air relative humidity, air dry-bulb temperature in the solar dryer chamber and bulk temperature of lemon were measured. Exhaust air temperature was measured by a sensor connected to a HOBO data-logger. The velocity of exhaust drying air was measured using (GENERAL No. DCFM700). Weight of fruit samples was recorded using an electrical digital balance with a maximum capacity of 600g, ± 0.01 g accuracy.

Mathematical Modeling

Thermal performance analysis without load

For many solar dryers system, air is an ideal media can be used to carry out moisture from agricultural products. Heat energy added and removed from this type of solar dryer unit by transport the medium itself (air), lead to minimize the temperature drop between transport fluid and drying chamber. The typical system in which air tank (solar greenhouse as a perfectly stirred tank) is used, can be represented by the solar air heating system. The heat energy balance on the solar dryer without load can be computed as follows (ASHRAE, 2011and Duffie and Beckman, 2013):

$$Q = Q_u + Q_{loss}, \quad \text{Watt} \quad (9)$$

The solar energy available inside solar dryer (Q) can be calculated in terms of the total solar radiation measured inside the dryer (R) in W/m^2 and net floor surface area (A_f) in m^2 as:

$$Q = R\,A_f, \quad \text{Watt} \quad (10)$$

The useful heat gain by dryer can be expressed in terms of the mass flow rate of drying air in kg/s, specific heat of air in J/kg ºC, and air temperature difference between indoor (T_{ai}) and outdoor (T_{ao}) in ºC as:

$$Q_u = m_a\,C_{pa}\,(T_{ai} - T_{ao}), \quad \text{Watt} \quad (11)$$

The thermal performance of the greenhouse type solar dryer is determined by its overall thermal efficiency (η_t) in converting solar energy into heat energy gain. The thermal efficiency is a combination of absorption efficiency and heat transfer efficiency.

$$\eta_t = \frac{Q_u}{R\,A_f}\,x\,100, \quad \% \quad (12)$$

The total heat losses from the inside solar dryer into the outside by conduction and convection (q_c), air exchange (q_e), and thermal radiation (q_r) can be computed from the following formula:

$$Q_{loss} = q_c + q_e + q_r, \quad \text{Watt} \quad (13)$$

The conduction and convection components can be calculated as follows:

$$q_c = U_o\,A_c\,(T_{ai} - T_{ao}), \quad \text{Watt} \quad (14)$$

Where, U_o, is the overall heat transfer coefficient in W/m^2 ºC and, A_c, is the net surface area of cover in m^2. The heat energy loss by forced air exchange can be computed by the following formula:

$$q_e = m_a\,C_{pa}\,(T_{ai} - T_{out}), \quad \text{Watt} \quad (15)$$

Where, T_{ai} and T_{out}, are the air temperature difference between inlet and outlet in ºC. The heat energy loss by thermal radiation can be computed as follows:

$$q_r = \varepsilon\,\tau\,\sigma\,A_f\left(T_{ai}^4 - T_s^4\right), \quad \text{Watt} \quad (16)$$

Where, ε, is the emissivity factor, τ, transmissivity factor for long-wave radiation, σ, Stefan-Boltzmann constant (5.669 x 10^{-8} W/m^2), and, T_s, ºK is the sky temperature in K. The sky temperature can be computed as follows:

$$T_s = 0.0552\,T_{ao}^{1.5}, \quad \text{K} \quad (17)$$

The normalized temperature rise of the solar dryer can be computed by the following relation:

$$D_T = \frac{(T_{ai} - T_{ao})}{R}, \quad \text{m}^2\,\text{ºC/W} \quad (18)$$

Heat Energy Balance

The energy balance is an important application to study the heat distribution in solar dryer (Fig. 4) and it's a mode to judge on the solar dryer system that use for drying process. The heat energy balance on the solar dryer comprises; energy balance on cover, inside air, and product (lemon). The energy balance on the cover is the thermal energy accumulated in the cover ($Q_{acc.}$) which equal the rate of thermal energy exchange between the air inside the dryer and the cover ($Q_{c,c\text{-}a}$) plus the rate of thermal energy exchange between the sky and the cover due to radiation ($Q_{r,c\text{-}s}$) plus rate of thermal energy exchange between the cover and ambient air due to convection (Q_w) plus rate of thermal energy exchange between the product and the cover due to radiation ($Q_{r,p\text{-}c}$) plus rate of solar radiation absorbed by the cover ($Q_{abs.}$). The energy balance on the cover can be interpreted as (Janjai, 2012):

$$\left[m_c\,C_{pc}\frac{dT_c}{dt}\right] = \left[A_c\,h_{c,c-a}(T_c - T_{ai})\right] + \left[A_c\,h_{r,c-s}(T_c - T_s)\right] + \left[A_c\,h_w(T_c - T_{ao})\right] + \left[\left[A_p\,h_{r,c-p}(T_c - T_p)\right]\right] + \left[A_c\,\alpha_c R_{out}\right] \quad (19)$$

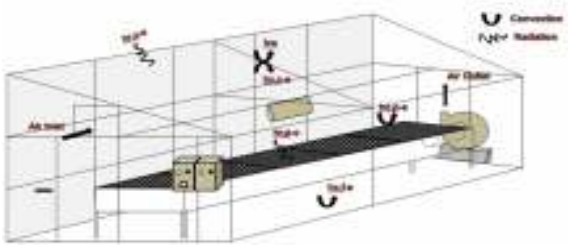

Fig. 4. Schematic diagram of energy transfer coefficient inside the solar dryer.

The energy balance on the indoor air is the rate of thermal energy gained by the air (Q_{aca}) which comprised the sum of; the rate of thermal energy exchange between the product and the air due to convection ($Q_{c,p\text{-}a}$), rate of thermal energy exchange between the floor and the air by convection ($Q_{c,f\text{-}a}$), useful heat energy gain by the solar drier during the drying process (Q_{gd}), rate of thermal energy gain by the air from the product due to the total thermal energy utilized for drying lemon (Q_{ev}), rate of overall heat loss from the dryer to the outdoor air (Q_{loss}), and rate of heat energy absorbed by the air inside dryer from solar radiation (Q_{abs}). The heat energy balance on the indoor air is:

$$\left[m_a\,C_{pa}\frac{dT_{ai}}{dt}\right] = \left[A_p\,h_{c,p-a}(T_a - T_p)\right] + \left[A_f\,h_{c,f-a}(T_a - T_f)\right] + \left[m_a\,C_{pa}(T_{out} - T_{ao})\right] + \left[h_{fg}\,m_w + m\,C_{pp}\,(T_{ai} - T_p)\right] + \left[U_c\,A_c(T_{ai} - T_{ao})\right] + \left[(1 - F_p)(1 - \alpha_f) + (1 - \alpha_p)\,F_p\,[A_c\,R_{in}]\right] \quad (20)$$

The approximated latent heat of vaporization of moisture in lemon can be approximated using the following equation developed by Gallaher, (1951):

$$h_{fg} = 2393.673\left(1 + 23\,e^{-0.40\,M\,(d.b.\%)}\right), \text{kJ kg}^{-1} \quad (21)$$

The specific heat of lemon can be determined as follows (Charm, 1971):

$$C_{pp} = 1.424\,M_c + 1.549 M_p + 1.675 M_f + 0.837 M_a + 4.187 M_m, \text{ kJ/kg ºC} \quad (22)$$

The energy balance on lemon fruits is the rate of thermal energy accumulated in the product (Q_{acp}) which equal the sum of; rate of thermal energy exchange between air and product due to convection ($Q_{c,p\text{-}a}$), rate of thermal

energy exchange between cover and product due to radiation ($Q_{r,p-c}$), rate of thermal energy utilized in drying process (Q_{ev}), rate of solar energy absorbed by the product (Q_{abs}). The heat energy balance on the product is:

$$\left[m_p\left(C_{pp}-C_{pl}M_p\right)\frac{dT_p}{dt}\right]=\left[A_p h_{cp-a}\left(T_a-T_p\right)\right]+\left[A_p h_{r,c-p}\left(T_c-T_p\right)\right]+\left[h_{fg}\,m_w+m\,C_{pl}\left(T_{al}-T_p\right)\right]+\left[F_p\,\alpha_p\,A_p\,R_{in}\right] \quad (23)$$

Radiation heat transfer coefficient between the cover and the sky ($h_{r,c-s}$) in W/m^2 K and between the product and cover ($h_{r,c-p}$) in W/m^2 K are computed (Duffie and Beckman, 2013) as:

$$h_{r,c-s}=\varepsilon_c\,\sigma\left(T_c^2+T_s^2\right)\left(T_c+T_s\right) \quad (24)$$

$$h_{r,p-c}=\varepsilon_p\,\sigma\left(T_p^2+T_c^2\right)\left(T_p+T_c\right) \quad (25)$$

Convective heat transfer coefficient (h_w) between the cover and the ambient air due to wind blowing over the cover in W/m^2 ºC, is calculated in terms of the wind speed, V_w, m/s as (Wattmuff and Charters, 1977):

$$h_w=2.8+3.0\,V_w \quad (26)$$

Convective heat transfer coefficient inside the solar greenhouse dryer for either the cover or product and floor (h_c), W/m^2 ºC is computed from the following relationship:

$$h_{c,f-a}=h_{c,c-a}=h_{c,p-a}=h_w=\frac{Nu\,k}{D_h} \quad (27)$$

Where, Nu, is the Nusselt number which can be computed from the following relationships (Holman, 2010):

$$Nu=0.0158\,Re^{0.8} \quad (28)$$

Where, Re, is the Reynolds number which is given by:

$$Re=\frac{D_h\,V_a\,\rho_a}{\upsilon} \quad (29)$$

Where, V_a, is the speed of the air in the dryer, ρ_a, is the air density, υ, is the viscosity of air and, D_h, is the hydraulic diameter and is given by:

$$D_h=\frac{4WD}{2(W+D)},\quad m \quad (30)$$

Data were measured and stored in microcomputer files and statistically analyzed using Excel program.

Examined drying models for simulating the drying data

The experiments data were employed to test the applicability of two studied thin layer models (Lewis's model and Henderson and Pabis's model) on describing and simulating the drying data. The exponential model (Lewis's model) is considered to be the simplest model to describe the moisture movement during drying agricultural products. The resistance to internal mass transfer is small as compared with the external resistance at the surface. Then it is assumes that the internal resistance of the product is negligible in comparison with the external resistance. It can be expressed as:

$$MR=\frac{M_t-M_e}{M_i-M_e}=\exp(-kt) \quad (31)$$

Henderson and Pabis's model is the development equation from simple model, the difference between the two models is that Henderson's model is considered the product shape by adding another constant as revealed in the following formula:

$$MR=\frac{M_t-M_e}{M_i-M_e}=A\exp(-kt) \quad (32)$$

The moisture ratio (MR = M_t/M_o) is replaced the (MR = $[(M_t-M_e)/(M_i-M_e)]$ for mathematical modeling of the solar drying curves due to the continuous fluctuation in temperature and the relative humidity of the drying air during solar drying process (Ayensu, 1997). The diurnal drying efficiency (η_d) is the ratio of energy required to evaporate the moisture from external surface of lemon to the surrounding media due to solar radiation flux incident and received over the surface area of the product.

$$\eta_d=\frac{Q_{ev}}{R\,A_p}\,x\,100,\quad \% \quad (33)$$

Regression analysis was proceeding using the statistical routine. Correlation coefficient (r) was one of the primary criterions for selecting the most appropriate equation to define the thin layer drying curves of the dried samples. The various statistical parameters such as; coefficient of determination (R^2) and standard error (SE) were used to determine the best model which can describe the solar drying behavior of lemon fruits. The best fit was decided for the highest value of (R^2) and minimum value of (SE).

RESULTS AND DISCUSION

Heating source (Solar energy)

Solar energy is the main source for heating drying air inside the solar dryer of lean-to greenhouse from and the drying process of lemon fruits during the experimental work. The outdoor solar energy available on a horizontal plane is the sum of two parts; beam radiation that directly received from the sun, and the diffuse radiation from the sky. Whilst, the indoor solar energy available is the sum of two parts; solar radiation transmitted through the glazing material of solar dryer, and the solar radiation reflected from the northern wall. During the experimental period, the hourly average solar radiation outside, inside, and reflected from the northern wall, respectively, were 518.8, 338.3, and 122.3 W/m^2. Consequently, the hourly average effective transmittance of solar dryer cover was 0.6521. It was varied from hour to hour according and day to another due to the solar incident angle which strongly affected the transmittance of glazing material. The hourly average reflectance factor of the northern wall inside the solar dryer was 0.3615. It also varied from hour to hour depending upon the solar azimuth angle which affected the reflectance factor. The hourly average solar radiation flux incident outside and inside the solar dryer with and without reflector and the contribution of reflector in increasing the intensity of solar radiation inside the dryer are listed in Table 1.

The hourly average solar radiation flux incident outside and inside with and without reflector during the first experiment was 518.8, 460.5, and 338.3 W/m^2, respectively. Consequently, the reflector increased the hourly average intensity of solar radiation by 36.3%. In reality, using the reflector led to increase the greenhouse effect phenomenon (thermal trapping) which contributed in rising the indoor air temperature.

For the duration of the first experiment, the daily average solar radiation flux incident outside, inside, and reflected from the northern wall, respectively, was 5.544, 3.602, and 1.313 kWh. There were obvious differences in daily average solar radiation recorded outside, inside, and reflected from the northern wall between the best day and daily average during the first experiment. These

differences were attributed to the effect of the atmospheric conditions. To evidently reveal the effect of effective transmittance of solar dryer glazing material and the atmospheric conditions on solar radiation flux incident inside the solar dryer, it was plotted against outside solar radiation (Fig. 5). The regression equation correlated the relationship between solar radiation inside and outside for the best fit was:

$$R_i = 0.6921\,(R_o) \quad R^2 = 0.8821 \quad (34)$$

Table 1. Hourly average solar radiation flux incident outside and inside with and without reflector and increasing percentage due to reflector during the first experiment.

Day		R_o, W/m^2	R_i With reflector, W/m^2	R_i Without reflector, W/m^2	Increasing percentage, %
21/8/2016	Mean	545.6	500.4	375.7	33.19
	SD	224.3	258.8	226.6	
22/8/2016	Mean	507.0	447.9	322.9	38.71
	SD	217.3	221.4	192.4	
23/8/2016	Mean	469.5	418.9	300.4	39.45
	SD	236.4	244.2	209.0	
24/8/2016	Mean	531.7	459.7	338.8	35.68
	SD	214.9	248.0	216.7	
25/8/2016	Mean	543.5	487.0	363.4	34.01
	SD	209.6	235.3	202.7	
26/8/2016	Mean	515.4	449.0	328.3	36.77
	SD	222.3	240.8	204.4	
Mean		518.8	460.5	338.3	36.3
SD		29.4	27.6	27.6	2.5

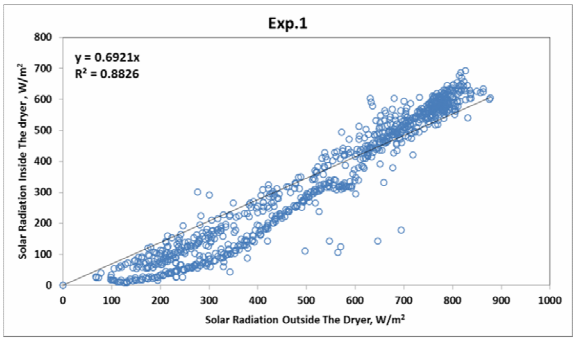

Fig. 5 Solar radiation flux incident outside the solar dryer against solar radiation inside during the experimental period.

The slope of equation is almost equal to the effective transmittance of the solar dryer glazing material. Some variations of the relative proportions of direct, diffuse, and ground-reflected components of solar radiation outside occurred. Thus scatter in some data of outside solar radiation were to be expected, because of atmospheric conditions. The relationship between the solar radiation reflected from the northern wall of the solar dryer and the solar radiation flux incident outside the solar dryer was examined (Fig. 6). Regression analysis revealed that, the relationship between them for the best fit was in a logarithmic function. Regression analysis also revealed a highly significant relationship (r = 0.8442; P = 0.001) between these parameters. The regression equation for the best fit under specific conditions during the first experiment was:

$$R_r = -258.95 + 62.267 \ln (R_o) \quad R^2 = 0.7126 \quad (35)$$

Regression analysis also revealed that, the most recorded scattering data occurred at early morning and prior to sunset due to the solar altitude angle, solar azimuth angle, and solar incident angle which strongly affected the reflected solar radiation.

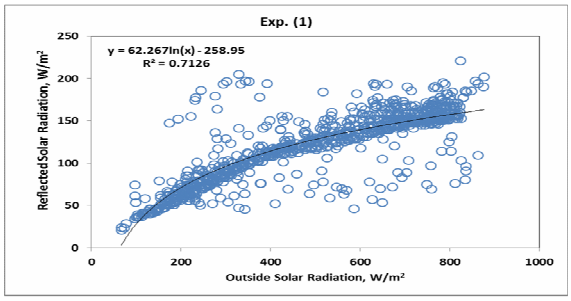

Fig. 6 Solar radiation reflected from the northern wall inside the solar dryer against solar radiation flux incident outside the dryer.

Ambient and drying air temperatures

The highest mean value of indoor air temperature (49.9ºC) was achieved in the day of 25/8/2016 whilst, the mean value of outdoor air temperature in the same day was 30.3ºC. Thus, the solar dryer increased the indoor air temperature over the outdoor by 19.6ºC. The highest mean value of lemon fruits bulk temperature (52.3ºC) was also realized in the same day due to reduction in moisture content of lemon fruits, accordingly, the majority of solar radiation consumed in rising the bulk temperature. For the duration of this experiment the daily average outdoor and indoor air temperatures, respectively, was 30.1 and 48.4ºC. Therefore, the lean-to greenhouse form increased the indoor air temperature over the outdoor by an average of 18.3ºC. The ability of solar dryer to raise the indoor air temperature over the outdoor and increasing percentage of air temperature rise during the experimental period is listed in Table 2. The maximum values of indoor (59.0°C) and outdoor (32.8°C) air temperatures were realized at 1.00 and 1.55 pm, respectively. The diurnal mean value of bulk temperature during this experiment was 48.7ºC whereas the mean value of indoor air temperature was 48.4°C. But after and before that times with insufficient or absent of heating source (solar radiation), the bulk temperature of lemon fruits could balance the indoor air temperature. To test and examine the influence of indoor air temperature (T_{ai}) on bulk temperature of lemon fruits (T_{bulk}) using solar energy technique, all the obtained data of bulk temperature under specific conditions was plotted against the indoor air temperature as illustrated in Fig. 7. Regression analysis revealed a highly significant linear relationship (r = 0.9423; P = 0.001). The best fit equations relating bulk temperature of lemon fruits with the indoor air temperature was:

$$T_{bulk} = -8.4427 + 1.1915\,T_{ai} \quad R^2 = 0.888 \quad (36)$$

Air relative humidity

Air relative humidity is in general the dominant parameters that affect drying process of any agricultural product. It plays an important role in carrying on the moisture evaporating from the agricultural product according to its capability to do that. As the air relative humidity is lowered under the moisture content of the agricultural product, its ability to carry on moisture increased. It has an inversely relationship with indoor air temperature particularly during daylight-time. The lowest mean value of indoor air relative humidity (24.72%) was realized in the day of 25/8/2016 whilst, the mean value of outdoor air relative humidity in the same day was

65.09%. Thus, the solar dryer lowered the indoor air relative humidity under the outdoor by 40.37%. The highest mean value of decreasing air relative humidity (40.80%) was achieved in the day of 24/8/2016. For the duration of this experiment the hourly average outdoor and indoor air relative humidity, respectively, was 67.31 and 28.38%. Therefore, the lean-to greenhouse form reduced the indoor air relative humidity under the outdoor by an average of 38.93%.

Table 2. Daily average outdoor and indoor air temperatures, and increasing percentage in air temperature during the first experiment

Day		T_{ao}, °C	T_{ai}, °C	Increasing percentage, %
21/8/2016	Mean	29.6	47.8	61.49
	SD	7.2	7.8	
22/8/2017	Mean	29.9	47.3	58.19
	SD	6.4	7.7	
23/8/2018	Mean	30.0	47.1	57.00
	SD	6.6	7.7	
24/8/2019	Mean	30.1	48.9	62.46
	SD	7.0	8.2	
25/8/2020	Mean	30.3	49.9	64.69
	SD	6.7	8.5	
26/8/2021	Mean	30.4	49.1	61.51
	SD	7.9	9.8	
Mean		30.1	48.4	60.90
SD		0.3	1.1	2.8

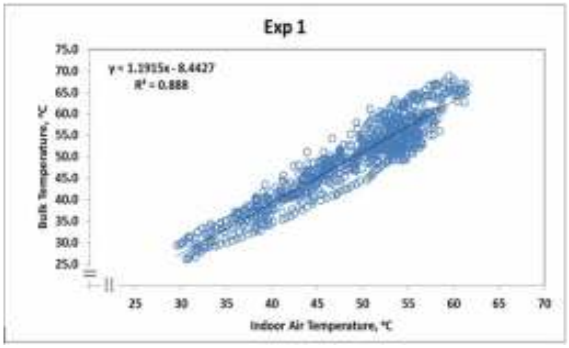

Fig. 7. Bulk temperature of Lemon fruits versus indoor air temperature during the first experiment.

Thermal Performance Analysis of Solar Dryer without load

Solar dryer was operated without load for three days (18-20/8/2016) prior to the experiment of drying process. The hourly average macroclimatic and microclimatic conditions during this period are summarized and listed in Table 3. The hourly average macroclimatic conditions included; solar radiation (R_o), air temperature (T_{ao}), and air relative humidity (RH_o) during this examination, respectively, were 548.8 W/m^2, 30.0ºC and 61.76%. Whilst, the microclimatic conditions comprised; solar radiation (R_i), air temperature (T_{ai}), temperature of expelled air (T_{ex}), and air relative humidity (RH_i) were 501.0 W/m^2, 49.2ºC, 57.2, and 22.52%, respectively. On the other hand, the hourly average microclimatic conditions comprised the total solar radiation inside the solar dryer (the sum of direct solar radiation and reflected from the northern wall), air temperature inside the dryer, temperature of expelled air from tray chamber, and air relative humidity during the experiment period, respectively, was 513.7 W/m^2, 49.9ºC, 58.1ºC, and 21.49%. This means that the solar dryer under these circumstances (without load) could raise the indoor air temperature by two modes. Firstly, when the outdoor air entered the solar dryer it was mixed with hot air of thermal trapping. Secondly, when the inside air passed through the tray chamber which painted from inside with matt black paint that has high absorptivity factor for solar radiation. The hourly average increasing percentage of indoor air temperature of the solar dryer over the outdoor was 64.69%, while, the hourly average increasing percentage of the expelled air temperature due to heat energy gained from different objects over the indoor air temperature was 16.43%. In reality, the solar dryer operated without load increased the indoor air temperature over the outside 91.75%. Because of all these reasons discussed above the solar dryer decreased the indoor air relative humidity as compared with the outdoor by 64.22%. To assess and examine the best model which may be used to correlate the input heat energy (hourly average solar energy incident inside the solar dryer with the hourly average output heat energy, all the obtained data were functioned in regression analysis as shown in Fig. 8. Regression analysis revealed a highly significant linear relationship with (r = 0.9518; P = 0.001). The regression equation for the best fit was:

$$Q_{output} = 0.8517\, Q_{input} + 8.5311 \quad (37)$$

Table 3. Macroclimatic and microclimatic conditions for the solar dryer operated without load.

Day		R_o	T_{ao}	RH_o	R_i	T_{ai}	T_{ex}	RH_i
18/8/2016	Mean	562.5	30.1	61.33	497.3	47.5	54.1	23.31
	SD	228.3	2.5	14.19	281.5	7.4	8.8	9.06
19/8/2016	Mean	541.4	30.0	62.92	503.1	50.0	58.8	22.69
	SD	237.1	3.1	14.83	270.5	8.0	11.8	9.34
20/8/2016	Mean	542.5	29.8	61.02	502.5	49.9	58.6	21.55
	SD	231.4	2.6	13.30	263.7	7.9	11.6	8.95
Mean		562.3	30.3	60.06	513.7	49.9	58.1	21.49
SD		224.4	2.3	12.22	265.1	7.1	10.3	7.98

The regression equation also reveals that, the output heat energy utilized 85.17% from the total input heat energy (solar radiation) and 14.83% from the total input solar radiation was reflected outside the dryer or accumulated as heat energy absorbed inside the solar dryer with the absent of solar radiation and this part represented by the value of y-intercept 8.531 kWh. The daily average input heat energy and the useful heat energy gained by the solar dryer during the period of experiment without load were 19.467 and 35 kWh, respectively. Useful heat energy gained during this experiment (without load) was plotted against the input heat energy (Fig. 9). Regression analysis revealed a highly significant linear relationship (r = 0.9429; P = 0.001). The regression equation for the best fit under specific conditions is:

$$Q_u = 0.5647\, Q \quad (38)$$

This regression equation also shows that, 56.47% of the total input heat energy was utilized in heating up the air entered the solar dryer and 28.7% of the total input energy absorbed by tray chamber, concrete floor, and structural frame. Also, the slope gives the overall thermal efficiency of the solar dryer without load under specific atmospheric conditions.

Thermal performance analysis of solar dryer with load

The daily average input heat energy (solar energy) and useful heat energy gain, respectively, was 34.689, 17.265 kWh for batch drying experiment. Regression

analysis revealed a highly significant linear relationship (r (batch) = 0.9472; P = 0.001) between input heat energy and useful heat energy gain (Fig. 10). The regression equation for the best fit under specific conditions was:

$$Q_u(batch) = 0.4857\ (Q) \quad (39)$$

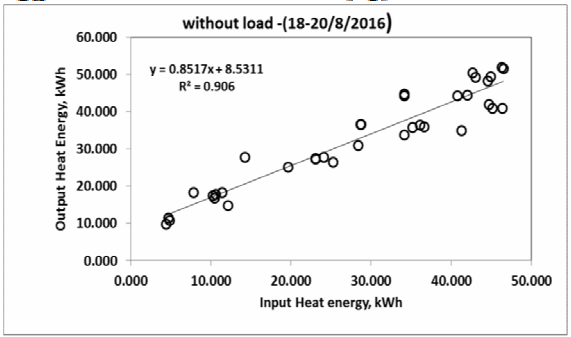

Fig. 8.Output heat energy as a function of input heat energy during the experimental period.

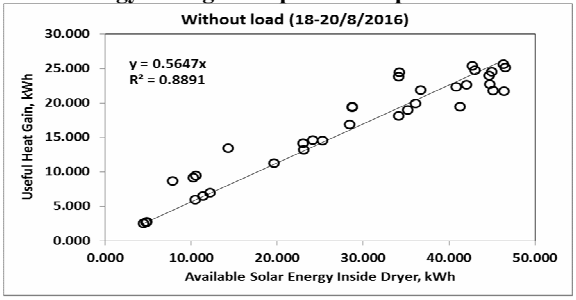

Fig. 9. Useful heat energy gain against input heat energy (solar energy) without load during the experimental period.

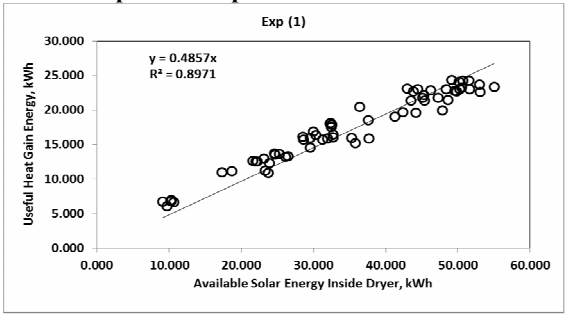

Fig. 10. Useful heat energy gain against input heat energy with load during batch and continuous drying processes, respectively.

It can be observed that, during the batch drying process there was 48.57% of the total input heat energy utilized as a useful heat energy gain and the rest 51.43% was absorbed by the drying product (lemon fruits), structural frame, concrete floor, tray chamber particularly with product (lemon fruits) shrinkage, and a part of reflected solar radiation from the northern wall was reflected into outside the solar dryer. The relationship between the overall thermal efficiency (η_o) and the normalized temperature rise (D_T) during the batch drying processes was examined and plotted in Fig. 11. The regression equation for the best fit was:

$$\eta_o = 44.065\ D_T \quad (40)$$

The slopes in these two linear equations represent the effectiveness of the solar dryer as a conventional heat exchanger which is defined as the ratio of the actual heat energy transferred to the maximum possible heat energy transferred. Therefore, this solar dryer type is diver from the other types which work as a solar collector such as tunnel solar dryer that the product is functioned as an absorber plate in the solar collector.

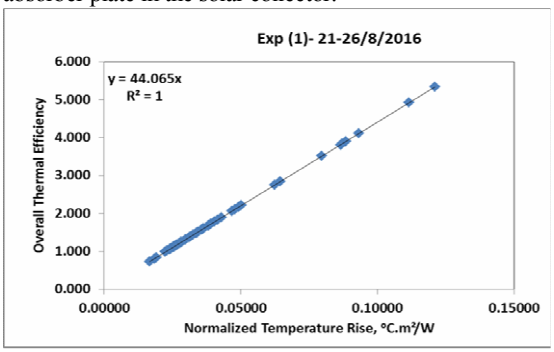

Fig. 11. Overall thermal efficiency against normalized temperature rise during the batch drying process.

Drying Behavior of Lemon fruits

Initial moisture content of lemon fruits varied depending on their color, skin thickness, and toughness. Dark green color lemon fruits have less moisture content and skin thicker and higher toughness. Yellow color lemon fruits have the highest moisture content and the lowest skin thickness and toughness. Light green color lemon fruits have a medium characteristic. Based on the previous characteristics, the moisture contents ranged from 80 to 90% (wb). Average initial moisture content for the three colors of lemon fruits was 87.04% ± 6.6% (wb) during this experiment. The final moisture content and the drying rate for the three different shapes of lemon fruits is summarized and listed in Table 4. The drying time for slices, half and whole lemon fruits, respectively, were 3 days (30 hours), 5 days (50 hours) and 6 days (60 hours).

Table 4. Final moisture content and drying for different shapes of lemon fruits during the first experiment

Experiment	shape	Final moisture content, % (wb)	Drying rate, kg/hr
Batch drying	Lemon	17.69	0.4202
	Half	17.38	0.2024
	Slices	17.30	0.1890
Control	Lemon	---	---
	Half	19.40	0.0175
	Slices	18.8	0.0233

Thus the slice was taken lower drying time, followed by half, and finally whole lemon fruits. While, in open sun drying (control experiment) drying times for slices and half were 14 days (140 hours) and 28 days (280 hours), respectively. On the other hand drying time for whole lemon fruits in open sun drying was 50 days without reaching safe final moisture content to storage, moisture content at the end of 50 days reached only to 50.19% with appearing of molds. It was difficult to compare between the drying rates of different shapes under the same experiment conditions because they had different initial weights. However, it can be compared the same shape under different experiments (batch and continuous drying process), due to the same initial weight. Changes in the moisture content (db) with drying time for slices, half and

whole lemon fruits during the first experiment are shown in Figs. 12, 13 and 14.

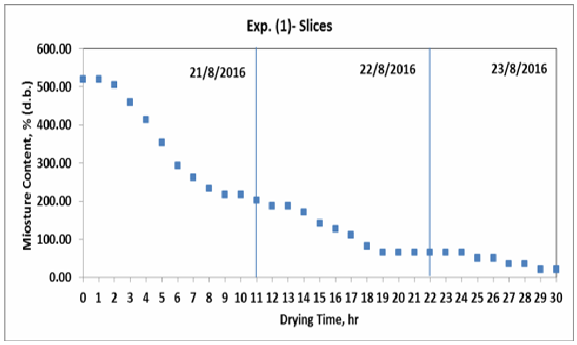

Fig. 12. Changes of slices moisture content with drying time for each day.

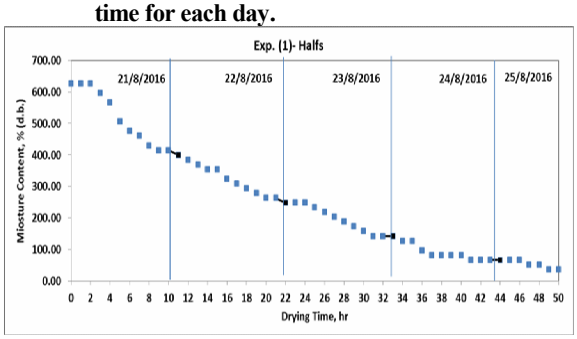

Fig. 13. Changes of half lemon moisture content with drying time for each day.

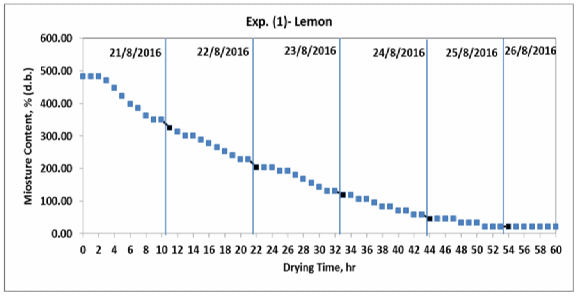

Fig. 14. Changes in moisture content for whole lemon fruits with drying time.

Thin layer drying models

Two models were functioned for data analyzing using Lewis and Henderson's models. All the data collected during this experiment for the three different shapes of lemon fruits (slices, half, and whole lemon fruits) were used in a simple regression analysis (Fig. 15) to examine the capability of these two models in analyzing the drying process. The regression analysis revealed a highly significant exponential relationship between these parameters. The regression equations for the best fit were:

MR_{LL}(For whole) $= \exp(-0.05\,t)$ (r=0.9717) (41a)

$MR_{HL} = 1.3861\exp(-0.058\,t)$ (r=0.9845) (41b)

MR_{LH}(For half) $= \exp(-0.05\,t)$ (r= 0.9822) (42a)

$MR_{HH} = 1.1964\exp(-0.55\,t)$ (r = 0.9885) (42b)

MR_{LS}(For slices) $= \exp(-0.096\,t)$ (r = 0.9850) (43a)

$MR_{HS} = 1.1471\exp(-0.103\,t)$ (r = 0.9879) (43b)

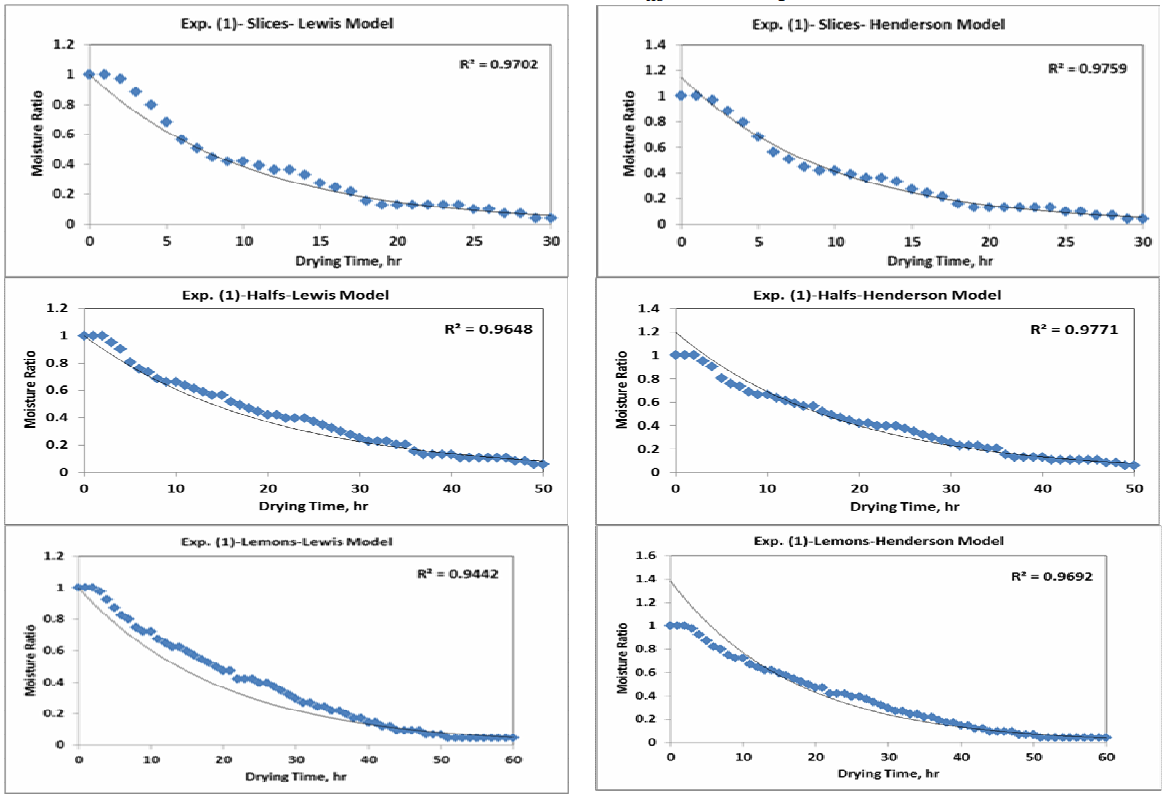

Fig. 15. Moisture ratio versus drying time for the three different shapes of lemon during the first experiment using Lewis and Henderson models.

The simple exponential equations described the experimental data of solar drying behavior for the three different lemon shapes with various moisture content showed a highly significant relationship between calculated and measured moisture content as revealed in Figs (16a) and (16b) during the experimental period. These simple models gave a satisfactorily drying behavior as evidently clarified from the coefficient of determination and standard error values listed in Table 5. Also, it can be observed that the Lewis's model had the highest coefficient of determination (R^2) values and the lowest standard error (SE) values for the three different shapes of lemon fruits as compared with Henderson's model. Thus, the Lewis's model has a good capability to represent the drying behavior of lemon using the solar lean-to greenhouse dryer under these circumstances.

Solar drying efficiency

The heat energy utilized in solar drying process varied from hour to hour and day to another during the experimental period according to the total solar energy incident inside the solar dryer and the moisture content of lemon fruits as listed in Table 6. It can be observed that, the diurnal average solar drying efficiency decreased from the highest value 29.09% in the first day till reached the lowest value 4.41% at the end of experiment due to reduction in moisture removed from lemon fruits. There are some negative values of sensible heat appeared in the first experiment particularly at the last three days after the drying process of lemon slices and half lemon fruits were accomplished. This causes increase in lemon bulk temperature than the drying air temperature due to absorption of solar radiation by tray chamber in this area.

Energy Balance on Solar Dryer

Energy balance on solar dryer cover

A combined regression analysis using data of heat energy input and output parameters clarified that the highest coefficient of determination (R^2 = 0.9058) was for the thermal heat energy transfer between the cover material and indoor air by convection and the lowest value (R^2 = 0.4799) was for the thermal radiation heat energy transfer between the cover material and product. This occurred because of the high indoor air temperature and the batch operation of the blower that cause simple movement for air by thermal buoyancy forces during switching off the blower. Thus the part of heat energy transfer between the cover material and the product by thermal radiation eradicated from the energy balance equation and the heat energy output being the sum of heat energy transfer between indoor air and the cover material by convection ($Q_{c,c-a}$), thermal radiation heat energy losses to the sky ($Q_{r,c-s}$) and convection heat energy losses due to wind speed (Q_w) as listed in Table 7. To assess and examine the best model which may be used to judge on solar drying types and to determine the heat energy accumulated in the cover material, all the obtained data was functioned in regression analysis as clearly clarified in Fig. 17. Regression analysis revealed a highly significant linear relationship (r = 0.9679; P = 0.001) between heat energy input and output. The regression equation for the best fit was:

$$Q_{input} = 0.6344\, Q_{output} + 13.988 \quad (44)$$

Table 5. Coefficient of determination (R^2) values and standard error (SE) values for Lewis and Henderson models during the first experimental period

Shape	Lewis Model		Henderson Model	
	R^2	SE	R^2	SE
Slices	0.9840	0.01574	0.9831	0.01777
Half	0.9875	0.01246	0.9779	0.01945
Whole	0.9792	0.01777	0.9542	0.02267

Table 6. Daily average solar energy available on tray (Q_a), sensible heat ($q_{sensible}$), latent heat (q_{latent}), total heat energy utilized in drying process (Q_{ev}), and Dryer efficiency during the first experiment

Day	Q_a, kWh	$q_{sensible}$, kWh	q_{latent}, kWh	Q_{ev}, kWh	η_{sd}, %
21/8/2016	3.787	0.122	0.980	1.102	29.09
22/8/2016	3.373	0.028	0.575	0.603	17.88
23/8/2016	3.184	0.003	0.437	0.440	13.81
24/8/2016	2.379	-0.002	0.296	0.294	12.34
25/8/2016	2.446	-0.003	0.132	0.129	5.25
26/8/2016	1.146	-0.001	0.051	0.051	4.41

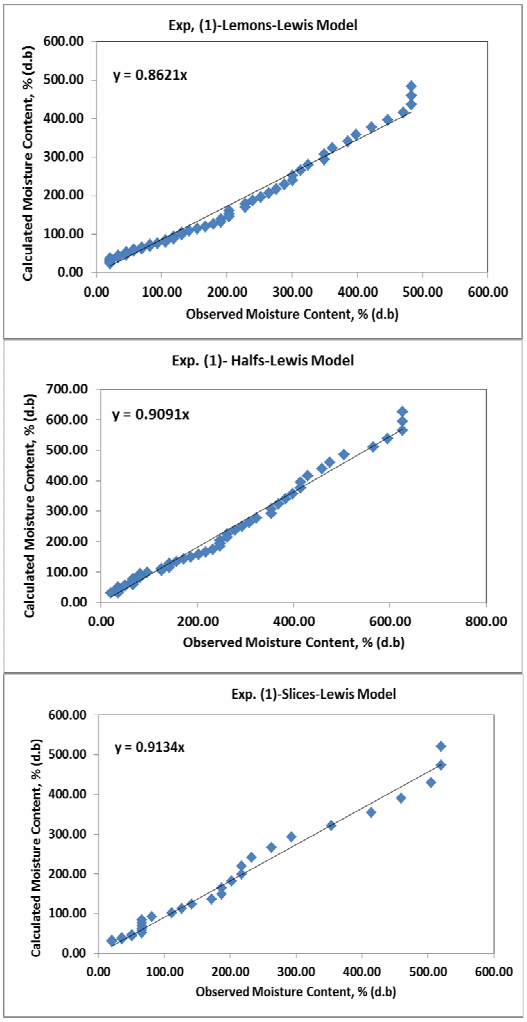

Fig. 16a. Validation of calculated moisture content with measured moisture content using Lewis model during the first experiment.

The regression equation also indicated that 63.44% of the cover material heat energy input transfer to indoor

and outdoor air by convection and to the sky by thermal radiation.

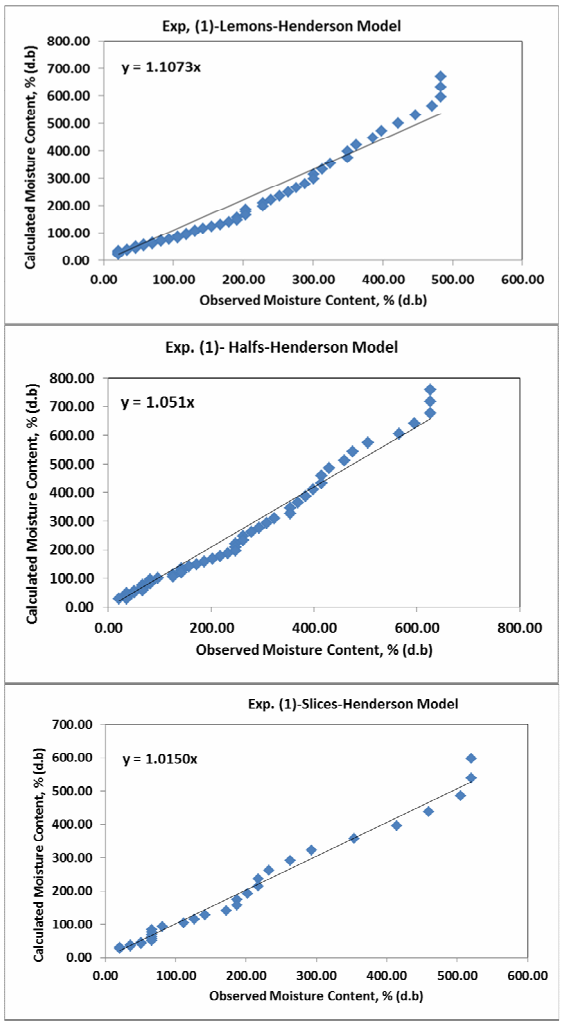

Fig. 16b. Validation of calculated moisture content with measured moisture content using Henderson model during the first experiment.

Table 7. Daily average heat energy input and output parameters for cover material during the first experiment.

Day	Q_{input}, kWh	Q_{output}, kWh			
	Q_{acc}	Q_{abs}	$Q_{c,c-a}$	$Q_{r,c-s}$	Q_w
21/8/2016	8.062	4.547	7.472	1.360	3.763
22/8/2016	8.062	4.215	8.136	1.347	3.723
23/8/2016	8.067	3.913	8.447	1.345	3.718
24/8/2016	8.086	4.421	7.396	1.383	3.847
25/8/2016	8.105	4.520	7.016	1.406	3.933
26/8/2016	8.096	4.281	7.667	1.387	3.859

Energy balance on the indoor air

The input and output parameters for indoor energy balance were listed in Table 8. It can be observed that, the convection heat energy between inside air and product was positive until the third day during the experimental period and thereafter, it had negative value. This because of shrinkage of lemon fruits that allowed solar radiation incident inside the tray chamber, thus lemon bulk temperature increased above the indoor air temperature.

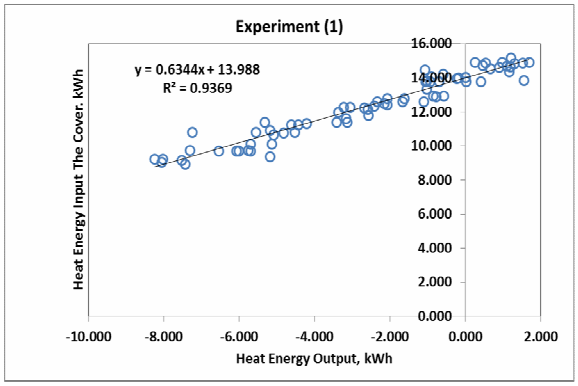

Fig. 17. Relationship between input and output heat energy for cover material.

Table 8. Daily average heat energy input and output parameters for drying air during the first experimental period.

Day	Q_{input}, kWh	Q_{output}, kWh				
	Q_{aca}	Q_{abs}	$Q_{c,a-p}$	Q_{gd}	Q_{loss}	Q_{ev}
21/8/2016	46.850	10.786	0.473	24.733	9.095	1.102
22/8/2016	46.343	9.607	0.162	22.890	8.697	0.603
23/8/2016	46.281	9.068	-0.532	22.279	8.557	0.439
24/8/2016	47.880	10.166	-0.107	24.143	9.391	0.294
25/8/2016	48.949	10.451	-0.316	22.450	9.820	0.129
26/8/2016	48.044	9.794	-0.411	22.711	9.325	0.065

The regression analysis between the heat energy output parameters and the heat energy input evidently revealed that, the highest coefficient of determination (R^2 = 0.9126) was for the heat energy gained by passing the indoor air through the solar dryer (Q_{gd}) and the lowest value (R^2 = 0.2315) was for the thermal heat transfer between indoor air and the product by convection ($Q_{c,a-p}$), and thermal energy utilized for drying lemon (Q_{ev}). Regression analysis clarified a highly significant linear relationship (r = 0.9532; P = 0.001) between heat energy input and output as shown in Fig. 18. The regression equation for the best fit was:

$$Q_{input} = 1.0707\, Q_{output} + 20.733 \quad (45)$$

This regression equation also revealed that, the heat energy input is represent 107.07% of the total heat energy output during this experiment.

Energy balance on the product (lemon fruits)

A combined regression analysis using data of heat energy output and heat energy input evidently clarified that, the convection heat energy between the indoor air and the product and the total thermal energy utilized for drying lemon fruits gave a highly coefficient of determination value (R^2 = 0.7220). This value was higher than that value for indoor drying air equation because in solar drying heating energy affecting both the drying air and the product temperatures, thus, the drying process depending on both. But the heat transfer between the product and the cover material due to thermal radiation had a weak effect on the energy balance. Therefore, it can be ignored from the equation of heat energy balance. To assess and examine the best model which described the relationship between input and output heat energy for the product, the obtained data of the batch drying mode was functioned in regression analysis as revealed in Fig. 19. Regression analysis revealed a highly significant linear relationship (r = 0.8716;

P = 0.001) between these parameters. The regression equation for the best fit was:

$$Q_{input} = 4.4696\, Q_{output} + 1.1675 \quad (46)$$

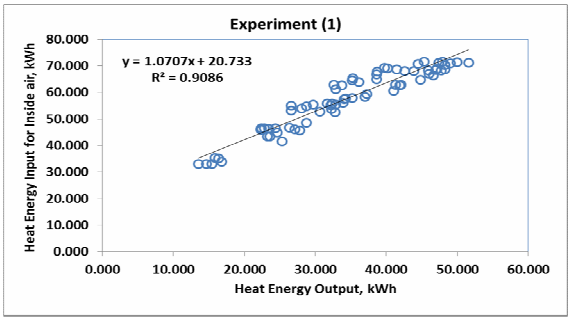

Fig. 18. Relationship between input and output heat energy for drying air during the first experimental.

The regression equation also indicated that, the heat energy input is represented 446.96% from heat energy output during the first experiment.

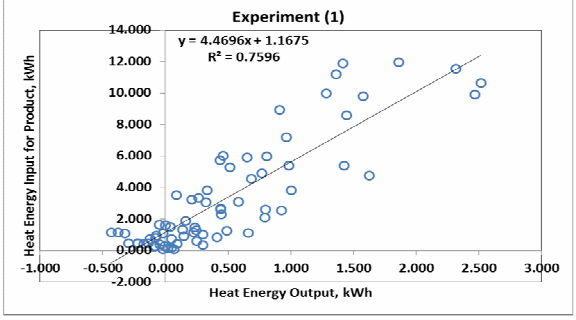

Fig. 19. Relationship between input and output heat energy for lemon fruits during the first experimental period.

CONCLUSION

Based on the results it can be concluded that reflector north wall can significantly increase the total solar radiation available inside the drier and indoor air temperature. Also, it was found that Lewis's model had the highest coefficient of determination (R^2) values and the lowest standard error (SE) values for the three different shapes of lemon fruits as compared with Henderson's model. Thus, the Lewis's model has a good capability to represent the drying behavior of lemon using the solar lean-to greenhouse dryer under these circumstances.

REFERENCES

Aravindh, M.; and Sreekumar, A., (2015) "Solar Drying – a sustainable way of food processing" Center of Green Energy Technology, Pondicherry University, Pondicherry 605014, India.

ASHRAE Handbook Fundamentals (2011) "American Society of Heating, Refrigerating and Air-Conditioning Engineers" SI Edition, Atlanta, GA30329, USA.

Ayensu, A. (1997) "Dehydration of food crops using a solar dryer with convective heat flow" Solar Energy; 59(4-6):12-16.

Belessiotis, V.; and Delyannis, E., (2011) "Solar drying" Solar Energy 2011:85:1665-

Charm, S.E., (1971)."Fundamentals of Food Engineering". 2nd edition. Avi publishing Co., Westport, Connecticut. (Cited in Heating and Cooling Engineering book by Matouk, A. M., (2006))

Chen, H.; Hernandez, C. E.; and Huang, T., (2005) "A study of the drying effect on lemon slices using a closed-type solar dryer" Solar Energy. 78:97-103.

Duffie, J. A. ; and Beckman, W. A. (2013) "Solar engineering of thermal processes" New York, N.Y.: John Wiley and Sons.

Gallaher, G. L. (1951) "A method of determining the latent heat of agriculture crop" Agriculture Eng., 32:34-38 (Cited by Hall C.W. *et al.,* 1980)

Holman, J. P., (2010) "Heat Transfer" Tenth edition. Published by The McGrow-Hill Companies Inc., 1221.

Jain, D.; and Tiwari, G. N., (2004) "Effect of greenhouse on crop drying under natural and forced convection, I: Evaluation of convective mass transfer coefficient" Energy Conversion Management, 45:765-783.

Janjai, S., (2012) "A greenhouse type solar dryer for small-scale dried food industries: Development and dissemination" International Journal of Energy and Environment, 3:3:383-398.

Kumar, M.; Sansaniwal, S.K.; and Khatak, P., (2016) "Progress in solar dryers for drying various commodities" Journal of Renewable and Sustainable Energy Reviews 55, 346-360.

Polygal, (2011) " Polygal polycarbonate multiwall sheets technical specifications" www.archplastics.com/wp-content/uploads/polygal-technical-guide pdf

Sharma, G. P.; Verma, R. C.; and Pathare, P. B., (2005) "Mathematical modeling of infrared radiation thin layer drying of onion slices" Journal of Food Engineering 71, 282-286.

Toshniwal, U.; and Karale, S. R., (2013)"A review paper on solar dryer". International Journal of Engineering Research and Application (IJERA) 3(2):896-9.

Watmuff, J. H.; and Charters, W. S. (1977) "Proctor D. Solar and wind induced external coefficients for solar collectors".

إستغلال بيت محمى كمجفف شمسى لتجفيف محصول الليمون. الجزء الأول:التجفيف الشمسى لليمون تحت درجة الحراره العالية.

صلاح مصطفى عبد اللطيف ، أحمد ثروت محمد وغادة على مسعد

قسم الهندسه الزراعيه- كلية الزراعة- جامعة المنصوره

الهدف الأساسى لهذا البحث هو تصميم وإنشاء وتقييم مجفف شمسى تجاري سعته تصل إلى 600 كجم لتجفيف محصول الليمون (من خلال التجفيف الشمسى على درجة حراره مرتفعه) وذلك فى منطقة التجارب بكلية الزراعه جامعة المنصوره لمشروع "تحسين جودة وكمية محاصيل البيوت المحميه بإستخدام الطاقة الجديده والمتجدده ونظم الزراعه الحيويه" عند خط عرض 31,04 شمالاً وخط طول 31,35 شرقاً وعند 6,72 م ارتفاع سطح البحر. ومن خلال هذه الدراسه تم تطبيق إحدى التقنيات الحديثه لزيادة الإحتباس الحرارى داخل المجفف التجارى على شكل بيت محمى مستند إلى حائط، حيث تم تغطية الحائط الشمالى بألواح من النيكل كروم بسمك 2 مم لتعمل كعاكس. وقد أظهرت النتائج أن إستخدام هذه التقنيه أدى إلى زيادة كمية الطاقه الشمسيه المتاحة داخل المجفف ودرجة حرارة هواء التجفيف بنسبة 36,30% و60,90% على الترتيب. تم تجفيف لليمون بأشكال مختلفه (شرائح, أنصاف, ليمون كامل) من محتوى رطوبى إبتدائى 87,04% على أساس رطب إلى 17,30%، 17,38%, 17,69% على أساس رطب فى 3, 5, 6 أيام خلال فترة التجفيف من 21 إلى 26 أغسطس لعام 2016.